A KNOWLEDGE-BASED APPROACH APPLIED TO AIRBORNE SAR IMAGES FOR CLASSIFYING LAND COVER/LAND USE IN THE BRAZILIAN AMAZON

C. M. Almeida [a, *], F. F. Delgado [b], R. A. S. Rosa [b], D. Luebeck [b], R. Q. Feitosa [c], G. A. O. P. Costa [c]

[a] INPE, Division for Remote Sensing, 12227-010 São José dos Campos – SP, Brazil - almeida@dsr.inpe.br
[b] OrbiSat da Amazônia S.A., Av. Shishima Hifumi, 2911- sala 404, São José dos Campos, SP, Brazil - (flavio.delgado, rafael, dieter.luebeck)@orbisat.com.br
[c] Pontifical Catholic University of Rio de Janeiro - PUC-Rio, Av. Marquês de São Vicente, 225, 22451-000, Rio de Janeiro, RJ, Brazil - (raul, gilson) @ele.puc-rio.br

KEY WORDS: OrbiSAR, Semantic Network, InterIMAGE, Semi-Automated Classification, Paragominas

ABSTRACT:

Land cover and land use mapping in rural environments of the Amazon from remotely sensed images is a challenging task in view of both the similar behavior of the concerned targets and also of the adverse climatic conditions, what often renders optical imagery practically useless for given periods of the year. The frequent presence of clouds in the region makes the use of SAR images a feasible alternative for the routine monitoring of both urban and rural domains, which is usually demanded by local urban and environmental planning and management authorities, farmers, ranchers, mining companies, and public and private enterprises dedicated to railways and roads construction. In most of the cases, SAR images are visually interpreted, what results in a time- and effort-consuming procedure. Conventional digital images processing techniques based on statistical properties extracted from the targets also present constraints, considering the confusion observed among rural land cover classes, such as between forest and natural secondary regrowth, riparian vegetation and forest, or culture and pasture. This work presents an alternative cognitive approach for classifying land cover and land use from airborne SAR images, based on the use of a hierarchical semantic network and fuzzy logic in InterIMAGE, an open source object-based platform designed for the interpretation of remote sensing images.

1. INTRODUCTION

Anthropic environments in the Brazilian Amazon usually consist of a set of fragmented targets of complex spatial patterns and confusing spectral behavior, comprising established urban settlements, periurban areas with bare soil and forest regrowth in different succession stages as well as agricultural and grazing plots amidst forest and savanna patches. Despite the challenges associated with the interpretation of such areas, a considerable amount of works in the peer-review literature have been dedicated to classify them.

Alves et al. (1999) conducted an analysis of landscape changes in a region of pioneer settlements in central Rondonia, western Brazilian Amazon, based on Landsat TM data. The authors concluded that in the time span considered for analysis (from 1977 to 1995), over 80% of the deforestation from 1985 to 1995 had occurred in regions within 12.5 km from areas of pioneer colonization deforested by 1977.

The use of spectral mixture linear analysis (SLMA) has also been strategically employed to classify land cover and land use in the Brazilian Amazon by Lu et al. (2002). In this work, the authors employed different processing routines on Lansat TM bands to map seven classes: mature forest, intermediate secondary succession (SS2), initial secondary succession (SS1), pasture, agriculture, water, and bare land (including urban areas, roads, and bare soil for cultivation). The selection of four endmembers (green vegetation, shade, bright soil, dark soil) and bands TM 3, 4, 5, and 7 provided the best classification result, attaining an overall accuracy of 86%.

Similar results have been obtained by Lu et al. (2004), who evaluated four different methods for classifying seven types of land cover classes in a western Brazilian Amazon study area, namely mature forest, advanced secondary succession, initial secondary succession, pasture lands, agricultural lands, bare lands, and water. The authors employed minimum-distance classifier (MDC), maximum likelihood classifier (MLC), extraction and classification of homogeneous objects (ECHO), and decision-tree classifier based on linear spectral mixture analysis (DTC-LSMA). DTC-LSMA and ECHO classifiers performed comparatively better, attaining an overall accuracy of 86% and 83%, and a Kappa index of 0.82 and 0.79, respectively.

In a further stage, Lu et al. (2007) decided to improve land cover classification accuracies in the Brazilian Amazon through different combinations of spectral signatures and textures from Landsat Enhanced Thematic Mapper Plus (ETM+) and Radarsat data. Optical and microwave data have been integrated by a wavelet-merging technique, and the MLC was applied based on the GLCM textures extracted with different sizes of moving window. The authors concluded that land-cover classification accuracies can be improved by the joint use of data fusion and texture metrics, and not by data fusion alone.

A high overall accuracy (0.92) was equally obtained by Carreras et al. (2004), who used multitemporal optical images from SPOT-4 VEGETATION and the probability-bagging classification tree (PBCT) to classify primary tropical forest, savanna, agriculture/pasture, water bodies, and secondary succession forest for the whole Brazilian Legal Amazon.

Mendoza et al. (2004), in a diverse approach from the previous works, used a unique non-parametric method - the unsupervised artificial neural network ART-2 (Adaptive Resonance Theory) - and ASTER images for land cover classification in a southern

* Corresponding author.

sector of the Brazilian Amazon. Nine classes were defined - crops, primary forest/ recently logged forest, degraded forest, secondary forest/bamboo, bare soil, straw covered soil, "clean" pasture, "overgrown" pasture, water, and the obtained overall accuracies for different bands combinations were rather lower, ranging from 68% to 69%.
A comparison of segment and pixel-based non-parametric land cover classification in the Brazilian Amazon was made by Brudeski et al. (2007) using multitemporal landsat TM/ETM+ imagery. These authors employed k-nearest neighbour (kNN) and classification and regression trees (CART) and both methods, when applied to multitemporal data, showed to perform equally well in the separation of just three classes: cleared, re-vegetated, and primary forest, with overall accuracies ranging from 77% to 91%, demonstrating the utility of inter-annual data for the given classes and region.
More recently, the use of data fusion relying on both optical and radar data as well as region-based analysis has predominated. This can be confirmed by the works of Silva et al. (2011) and Walker et al. (2011). The former authors conducted an analysis employing separated and pan-sharpened Landsat5/TM and ALOS/PALSAR images, using a region-based classifier based on the Bhattacharyya distance. The authors concluded that for the 10 analysed classes, the TM data alone is better to classify land cover classes with occurrence of trees or shrubs, while SAR data contribute to improve the classification results in low vegetated areas. Walker et al. (2011) used the Definiens platform to comparatively evaluate the performance of Landsat/TM and ALOS/PALSAR (HH and HV) images for a large area classification in the Brazilian Amazon. Different classes detailing levels were employed (15, 10, 7, 6, and 2 classes), and overall accuracy varied as a function of both the total number of classes and of variables considered for classification, ranging from 39.2% in the case of PALSAR (13 variables and 15 classes) to 89.5% in the case of Landsat (49 variables and 2 classes).
According to what was previously exposed, it is to be concluded that OBIA is still to a very limited extent explored for land cover and land use classification in the Amazon. Considering this fact, this work is committed to present an alternative cognitive approach for classifying land cover/use from airborne SAR images, based on the use of a hierarchical semantic network and fuzzy logic in InterIMAGE, an open source object-based platform designed for the interpretation of remotely sensed images.

1.1 System Description

InterIMAGE is based on the software GeoAIDA (Bückner et al., 2001), developed at the TNT Institute of the Leibniz Hannover University, Germany, and it inherited from that system the basic functional design, knowledge structures, and control mechanisms. A new graphical user interface, a knowledge model debugging tool, multitemporal interpretation capability and some image processing operators are also available at InterIMAGE.
In short, InterIMAGE implements a specific image interpretation strategy. Such strategy is based upon and guided by a hierarchical description of the interpretation problem, structured in a semantic network.
The bases for interpretation of digital image data are the results generated by image processing operators. In this context, an image processing operator is any operator that generates a labeled result image of a given image. Such image processing operators are denoted here as 'classifying operators'. They can fulfill threshold operations, texture-based or model-based methods and build the basis for the interpretation of a scene.
In most of the systems that use semantic networks for knowledge representation, only the leaf nodes of the network can be associated to image processing operators. The following grouping of the objects often produces a very high combinational diversity, because all objects extracted from the image have to be taken into account at the same time.
In InterIMAGE, holistic operators (Liedtke et al., 1997) can be used to reduce the combinatory diversity problem. Holistic operators aim at identifying specific types of objects independently of the identification of their structural components. They can be connected to any node of the semantic network, and their basic task is to divide a region into sub-regions, reducing the need of processing alternative interpretations. The structural interpretation of the sub-regions that follows can verify or disprove the holistic results.
Moreover, InterIMAGE permits the integration of any of such classifying operators in the interpretation process. The problem that different operators can generate different information for the same region in the image is solved by the use of additional knowledge regarding the judgment of the competing interpretations. Furthermore, as different operators can process different types of data, the system permits the integrated analysis of image and GIS data from multiple sources.

1.2 Interpretation Strategy

In InterIMAGE explicit knowledge about the objects expected to be found in a scene is structured in a semantic network, defined by the user through the system's graphic user interface (GUI).
A semantic network contains nodes and edges, whereat nodes represent concepts and edges represent the relations between the concepts. The network is actually a connected graph with no cycles, i.e. a tree. In each concept node, information necessary for the analysis, such as the image processing operator specialized in the search of occurrences of the concept, is defined. During the analysis, guided by the semantic network, the system controls the execution of the operators and generates a network of instances, each instance defining a geographic region associated to a specific concept.
Interpretation of remote sensing data means to transform input data into a structural and pictorial description of the input data that represents the result of the analysis. In InterIMAGE, the result of the interpretation contains a structural description of the result (network) and thematic maps. The final and all intermediate results (region descriptions), are stored in XML format, and can be used for further external examinations.
The analysis process performed by InterIMAGE has two steps: a bottom-up and a top-down one. The top-down step is model-driven and generates a network of hypotheses based on the semantic network. The grouping of hypotheses and their acceptance or refusal is a task of the data-driven bottom-up analysis. The final instance network results from the bottom-up data-driven analysis.
In each node of the network the user defines the information necessary for the execution of each processing step, that is, the image processing (classifying) operator and respective parameters to be used in the top-down step (top-down operator) as well as the decision rules to be used in the bottom-up step.
The top-down operators are entrusted with separating regions into sub regions and with building hypotheses for the concepts of the semantic network, regions of the image associated to the concepts. This task is realized recursively from the root to the leaf nodes. For this purpose any (external) image processing

operator, which creates hypotheses for the sub region, can be used in the analysis process.
When the top-down analysis reaches the leaf nodes, the interpretation turns from model-driven to data-driven (bottom-up). The decision rules for the bottom-up step are defined in a particular stack-based language that provides functions for deciding between spatially concurrent hypotheses generated in the top-down step.

2. STUDY AREA

The selected study area concerns Paragominas city (municipal seat) and its rural surroundings, situated in the northern State of Pará, Brazil (Figure 1). The city is located approximately at latitude S 02° 59' 45" and longitude W 47° 21' 10", with an average elevation of 90 m above sea level. The municipality extends over a surface of 19,395.69 km² and comprises a population estimated at 97,788 inhabitants in 2010. Its main economic activities are the exploitation of bauxite and logging.
The SAR images of this area were acquired with the OrbiSAR sensor, produced by the Brazilian enterprise OrbiSat, for bands P (~ 0.60 - 1.2 m) and X (~ 2.5 - 3.75 cm), with a radiometric resolution of 32 bits, and a spatial resolution of 2.5 m. The aerial survey was carried out from February 11th to March 13th, 2007, with a flight height of 11,000 m and in the E-W direction.

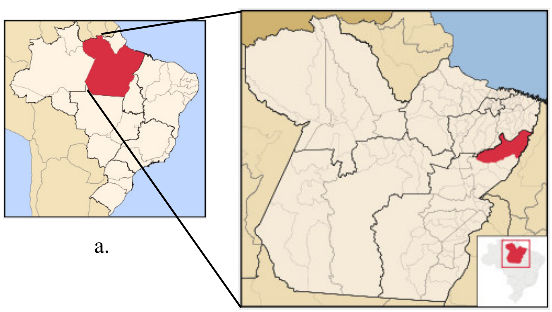

a. b.

Figure 1. Study area: a. Brazil with Pará state in red b. Pará state with Paragominas municipality in red

The selected original scene was cut for the interpretation experiment (Figure 2), and its dimension resulted in 2,641 lines and 2,367 columns. The sub-scene included all types of land cover/use classes contained in the original scene, so as to comprise the diversity and challenges found in the image.

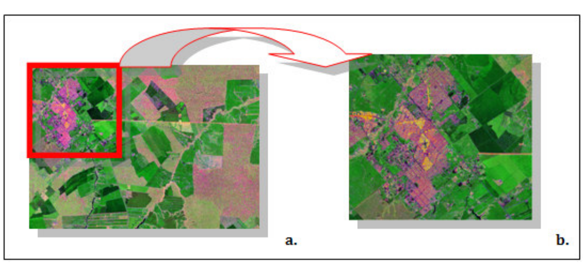

Figure 2. Study area: a. Original scene of Paragominas image – RGB composition using P and X amplitude images and Data Range of P b. Sub-scene used for interpretation, with Paragominas city at the centre, in the same color composition
Source: Adapted from OrbiSat (2007a)

3. METHODS

3.1 Data Acquisition and Pre-processing

At the time this classification experiment was accomplished, InterIMAGE could only support the processing of images with 8 bits of resolution. Although the OrbiSAR images were acquired with 32 bits, this experiment only employed images degraded to 8 bits. This constraint has been overcome in the latest versions of InterIMAGE.
The SAR images had been already orthorectified by OrbiSAR and presented in all cases a resolution of 2.5 m, as previously stated. Initially, tests were conducted with different filters available at ENVI 4.5, in which the Frost filters demonstrated to yield the best results for the envisaged classification.
Frost filters are commonly used to remove speckle, a noise inherent to the imaging due to the coherent nature of a SAR (Synthetic Aperture Radar) sensor. These filters are able to remove such noise and at the same time preserve the targets edges in the images. They operate as circularly symmetric filters of exponential decay, based on local statistical metrics. Each filtered pixel is replaced by a calculated value considering the distance to the filter center, a decay factor, and the local variance (ITTVIS, 2008).
After applying Frost filters, input bands for segmentation and classification were produced based on the filtered images, on the application of some texture metrics, and also on a Principal Components Analysis transform, which input bands are listed in Table 1.

Code	Input Band
P	P band (amplitude)
X	X band (amplitude)
DRP	Data range of P band (3x3 filter and digital number – DN – occurrence measures)
DRX	Data range of X band (3x3 filter and DN occurrence measures)
Var P	Variance of P band (3x3 filter and DN occurrence measures)
Var X	Variance of X band (3x3 filter and DN occurrence measures)
Diss P	Dissimilarity of P band (3x3 filter and DN co-occurrence measures)

Table 1. Input bands of the PCA transform

Further information on the calculation of Data Range, Variance and Dissimilarity can be found at ENVI software user guide (ITTVIS, 2008).
Besides the PCA transform, a customized attribute has also been created based on the sum of the following four bands:

i) standard-deviation of the variance of X band (3x3 filter and DN occurrence measures);
ii) standard-deviation of the variance of X band (3x3 filter and DN co-occurrence measures);
iii) standard-deviation of the dissimilarity of X band (3x3 filter and DN co-occurrence measures);
iv) standard-deviation of the 4^{th} PCA band.

3.2 Land Cover and Land Use Classes and Reference Map

The adopted land cover and land use classes were based on a thematic map manually issued by a team of expert photo-interpreters working for the images producer (OrbiSat, 2007b), comprising eight classes: natural secondary regrowth, forest, riparian vegetation, bare soil, pasture/grasslands, cropland, water bodies (lakes, lagoons, dams), and urban areas. Linear features and minor targets, like narrow rivers, paved and non-paved roads, fences, paths, railways, transmission lines, and buildings, were disregarded in the semiautomatic interpretation procedure reported in this paper.

4. EXPERIMENT DESIGN: OBJECT-BASED CLASSIFICATION

An initial interpretation strategy was observed in this classification experiment so as to obtain a segmentation as close as possible to the real boundaries belonging to the targets of interest. In none of the segmentation results preliminarily produced, it was possible to have the frontiers of the urban settlement correctly delimited, i.e., without the inclusion of other land cover/land use classes. This would render unfeasible the elaboration of a semantic network meant to initially separate urban and non-urban classes, since both of these superclasses would be considerably contaminated by each other. For this reason, the design of the final semantic network kept all land cover/land use classes at the same level, immediately below the node responsible for solving conflicts among classes and executing the final classification (Paragominas node), located right underneath the Scene node, to which all other nodes are subjugated (Figure 3).

In this solution, the unique segmentation produced strived to preserve the frontiers of interest, and hence, it was possible to eliminate unnecessary complexities in the semantic network represented by subclasses of commission errors in the subsequent nodes (and respective segmentations), besides the fact that the generated segments presented appropriate sizes for feature extraction.

The best segmentation result was based on three input bands: data range of X band, and the X and P bands subject to the Enhanced Frost filter, each of them being equally assigned weight 1.0. The value of 290 was employed for scale factor, 1.0 for compactness parameter, and 0.7 for shape parameter (Baazt and Schäpe, 2000). Although the produced segmentation was considered satisfactory, minor adjustments were executed by means of vector edition, aiming to ensure as much as possible the similarity between the segments frontiers and the boundaries of real targets. This procedure did not take longer than 15 minutes and altered the shape of about 30 segments, either splitting or merging them. A comparison between the original

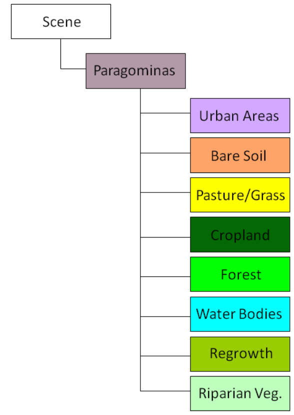

Figure 3. Semantic network for land cover and land use classification in Paragominas

and the edited segmentation is presented in Figure 4. The vector edition was accomplished in ArcGIS 9.2, and the resulting shape file was reimported in InterIMAGE, being reused as an input layer for segmentation through the command *Shape File Import*.

The reduced separability among the concerned classes became clear when attributes started being spatialized for the generated segments using the *Feature Viewer* comand, available at the menu *Spatial Analysis Explorer* of InterIMAGE. This limited separability can be ascribed to the following reasons:

- SAR images do not provide information on the targets spectral behavior, i.e. the way by which their physical-chemical properties influence the mode they will interact and backscatter the incident electromagnetic radiation.
- The OrbiSAR sensor operates with bands P and X. All the information used for classification is solely derived from these two bands, which capture geometric and not spectral information, although physical parameters, like the dielectric constant, interfere in the targets backscattering.
- The use of 8 bits images instead of 16 or 32 bits implies a sharp reduction in information, what makes all land cover/use classes more similar to each other, and hence, less separable.
- The adopted land cover and land use classes by OrbiSat (2007b) already present similar backscattering response, as in the case of bare soil and pasture/grasslands, of forest and natural secondary regrowth, and of cropland and bare soil.

a. b.

Figure 4. a. Original segmentation of study area b. Edited segmentation, with red ellipses indicating some areas of change

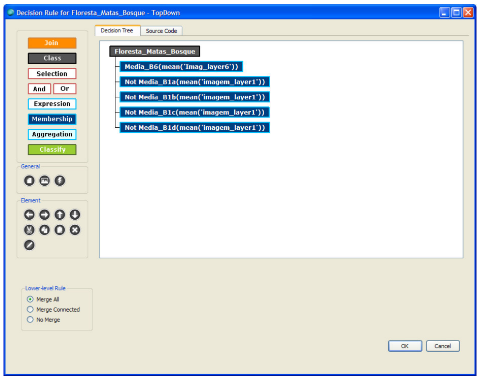

a.

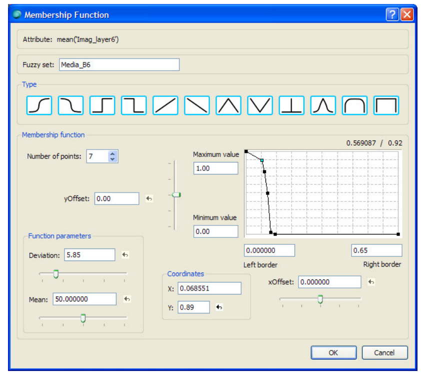

b.

Figure 5. a. Set of attributes used to discriminate forest b. Fuzzy membership curve related to the mean of the X band homogeneity (band 6)

- Texture metrics in SAR images are suitable for discriminating land cover and land use classes. However, with 8 bits of radiometric resolution and mostly operating with the mean of large segments, it turns out that all the richness and diversity of information content is practically lost. An ideal solution would be to operate with the standard-deviation of texture metrics, what is operationally unfeasible, unless this would be generated in a separate environment, such as a GIS platform.

Based on the semantic network presented in Figure 3, the characterization of the class **forest** took into account two attributes: the negative of the P band mean and the mean of the X band homogeneity (Figure 5), considering the co-occurrence of DN. The **natural secondary regrowth** was also based on two attributes: the negative of the X band mean and the standard-deviation of the X band previously subject to the Enhanced Frost filter. **Riparian vegetation** considered two attributes derived from the PCA transform: the negative of the 1st PCA band mean (crisp curve) and the mean of the 1st PCA band (fuzzy curve). **Bare soil** was extracted by means of the second angular moment of the P band previously subject to the Enhanced Frost filter as well as of the negative of the P band mean. **Cropland** was identified based on the negative of the standard-deviation of the 1st PCA band and by the mean of the 6th PCA band. **Water Bodies**, on their turn, were discriminated by the negative of the P band mean, the standard-deviation of the X band entropy, considering the occurrence of DN, and the negative of the standard-deviation of the 1st PCA band. **Pasture** was characterized by the mean of the X band variance, considering the occurrence of DN, and by the negative of the P band mean. Finally, **urban areas**, which reliability parameter was superior to all other classes, were discriminated based on two attributes: the negative of the P band mean and a customized attribute derived from a sum of four bands, explained in Section 3.1.

5. RESULTS AND DISCUSSION

Figure 6 shows the classification result compared to the thematic map produced through visual interpretation by OrbiSat (2007b). In total, five objects were wrongly classified and were reassigned to their true classes by means of manual edition. Some problems identified in the interpretation process resulted directly from the fact that the selected study area is in fact an inset of a scene. This is the case of the class forest, which owns only two polygons (segments) located in the upper and lower right edge of the scene. For this reason, the attributes and respective thresholds for such class are somehow biased

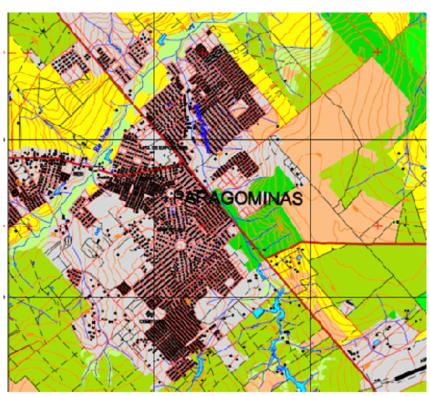

b.

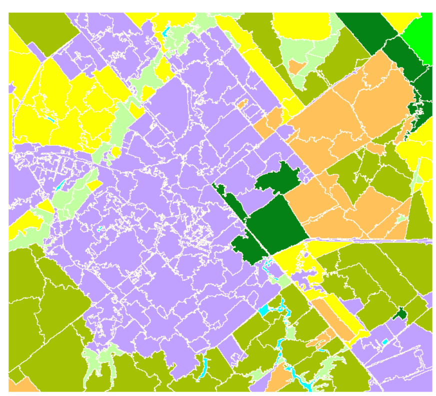

b.

Figure 6. a. Inset of the thematic map (reference map) manually executed by photo-interpreters of OrbiSat (2007b) and containing the study area b. Final classification result for the study area produced by InterIMAGE (Color legend is found in Figure 3)

CLASSES		References								Total
		A	B	C	D	E	F	G	H	
Classification	A - Urban Areas	**136**	4	1	3	2	2	1	6	155
	B - Bare Soil	2	**54**	0	2	0	0	0	1	59
	C - Pasture/Grasslands	2	1	**64**	1	0	1	1	3	73
	D - Cropland	0	0	0	**32**	0	0	1	0	33
	E - Forest	0	0	0	2	**17**	0	0	0	19
	F - Water Bodies	0	0	0	0	0	**18**	0	1	19
	G - Natural Secondary Regrowth	8	0	2	0	0	8	**71**	2	91
	H - Riparian Vegetation	2	1	3	0	1	1	6	**37**	**51**
	Total	**150**	**60**	**70**	**40**	**20**	**30**	**80**	**50**	**500**
	Global Accuracy: 0.8580				**Kappa Index : 0.8277**					

Table 2. Errors matrix and agreement indices for the object-based classification of land cover and land use

given the reduced number of samples within the study area. Other problems relate to small lakes which were not detected by segmentation, besides spurious boundaries of riparian vegetation, which present a very complex shape. For validating this classification, 500 random points, collected through stratified sampling based on the share of each class area, were taken into account. The validation results are presented in Table 2, indicating a reasonable amount of omission errors of urban areas (wrongly classified mostly as riparian vegetation, bare soil, and cropland) as well as of riparian vegetation, mainly due to segmentation problems. The global accuracy achieved 86% and the Kappa index reached 83%, what is regarded as a very good accuracy accordingto a ranking of Landis and Koch (1977).

6. CONCLUSIONS

It is worthy emphasizing that SAR images with 8 bits of radiometric resolution do not represent the ideal input data for classification, considering that the often use of a mean value for a given attribute seriously hinder the objects separability. On the other hand, SAR images are extremely suitable for segmentation, since the geometric information acquired by active sensors pretty well detects the targets boundaries in the scene. The high classification accuracy obtained in this experiment was not only derived from the semantic net and its respective attributes and thresholds, but also and mainly from the correct definition of the targets frontiers during segmentation. Future works dealing with higher radiometric resolution (16 and 32 bits) are envisaged.

REFERENCES

Alves, D. S., Pereira, J. L. G., de Sousa, C. L., Soares, J. V., Yamaguchi, F., 1999. Characterizing landscape changes in Central Rondônia using Landsat TM imagery. *International Journal of Remote Sensing*, 20(14): pp. 2877-2882.

Baatz, M., Schäpe, A., 2000. Multiresolution segmentation—an optimization approach for high quality multi-scale image segmentation. In: Strobl, J., Blaschke, T., Griesebner, G. (Eds.), *Angewandte Geographische Informations-Verarbeitung XII*, Wichmann Verlag, Karlsruhe, pp. 12-23.

Brudeski, K. A., Wynne, R. H., Browder, J. O., Campbell, J. B., 2007. Comparison of segment and pixel-based non-parametric land cover classification in the Brazilian Amazon using multitemporal Landsat TM/ETM+ imagery. *Photogrammetric Engineering and Remote Sensing*, 73:(7) pp. 813-827.

Bückner, J., Pahl, M., Stahlhut, O., Liedtke, E.-C., 2001. geoAIDA - A knowledge-based automatic image data analyser for remote sensing data. In: *The Second International ICSC Symposium on Advances in Intelligent Data Analysis - CIMA 2001*, Bangor, Wales, United Kingdom.

Carreiras, J. M. B., Pereira, J. M. C., Campagnolo, M. L., Shimabukuro, Y. E., 2005. A land cover map for the Brazilian Legal Amazon using SPOT-4 VEGETATION data and machine learning algorithms. In: *Brazilian Symposium on Remote Sensing*, Goiânia (GO), Brazil.

ITTVIS, 2008. *ENVI 4.5: ENVI Help*. ITT Visual Information Solutions, Washington, D.C., EUA.

Landis, J., Koch, G., 1977. The measurement of observer agreement for categorical data. *Biometrics*, 33(1), pp. 159-174.

Liedtke, C.-E., Bückner, J., Grau, O., Growe, S., Tönjes, R., 1997. AIDA: A System for the Knowledge-Based Interpretation of Remote Sensing Data. In: *Third International Airborne Remote Sensing Conference and Exhibition*, Copenhagen, Denmark.

Lu, D., Batistella, M., Moran, E., 2002. Linear spectral mixture analysis of TM data for land-use and land-cover classification in Rondônia, Brazilian Amazon. In: *Symposium on Geospatial Theory, Processing and Applications*, Ottawa, Canada.

Lu, D., Batistella, M., Moran, E., 2007. Land-cover classification in the Brazilian Amazon with the integration of Landsat ETM+ and RADARSAT data. *International Journal of Remote Sensing*, 28(4): pp. 5447-5459.

Lu, D., Mausel, P., Batistella, M., Moran, E. F., 2004. Comparison of land-cover classification methods in the Brazilian Amazon Basin. *Photogrammetric Engineering and Remote Sensing*, 70(6): pp. 723-731.

Mendoza, E.H.R.; Santos, J.R.; Santa Rosa, A.N.C.; Silva, N.C., 2004. Landuse/land cover mapping in Brazilian Amazon using neural network with ASTER/TERRA data. In: International Society for Photogrammetry and Remote Sensing Congress, Istanbul, Turkey, Vol. XXXV, Part B, pp. 123-127.

OrbiSat da Amazônia Ind. e Aerolevantamento S. A., 2007a. *Paragominas Images (PA)*. Sensor OrbiSAR. Bands X and P. CD-ROM. OrbiSat, Campinas, SP.

OrbiSat da Amazônia Ind. e Aerolevantamento S. A., 2007b. *Planialtimetric Mapping by Interferometric Radar*. Sheet 235-659. Scale 1:25,000. OrbiSat, São José dos Campos, SP.

Silva, W. B., Pereira, L. O., Sant'Anna, S. J. S., Freitas, C. C., Guimaraes, R. J. P. S., Frery, A. C., 2011. Land cover discrimination at Brazilian Amazon using region-based classifier and stochastic distance. In: *Geoscience and Remote Sensing Symposium (IGARSS)*, Vancouver, Canada, pp. 2900-2903.

Walker, W. S., Stickler, C. M., Kellndorfer, L. M., Kirsch, K. M., Nepstad, D. C., 2010. Large-area classification and mapping of forest and land cover in the Brazilian Amazon: a comparative analysis of ALOS/PALSAR and Landsat data sources. IEEE Journal of Selected Topics in Applied Earth Observations and Remote Sensing, 3(4): pp. 594-604.